THE JOURNAL OF PHYSICAL CHEMISTRY A

Article

pubs.acs.org/JPCA

Structural Rearrangements and Magic Numbers in Reactions between Pyridine-Containing Water Clusters and Ammonia

Mauritz J. Ryding,*[,†] Kai Ruusuvuori,[‡] Patrik U. Andersson,[§] Alexey S. Zatula,[†] Matthew J. McGrath,[∥] Theo Kurtén,[‡] Ismael K. Ortega,[‡] Hanna Vehkamäki,[‡] and Einar Uggerud*[,†]

[†]Mass Spectrometry Laboratory and Centre of Theoretical and Computational Chemistry, Department of Chemistry, University of Oslo, P.O. Box 1033 Blindern, NO-0315 Oslo, Norway

[‡]Division of Atmospheric Sciences, Department of Physics, University of Helsinki, P.O. Box 64, FI-00014 University of Helsinki, Helsinki, Finland

[§]AstraZeneca R&D Mölndal, Pepparedsleden 1, SE-431 83 Mölndal, Sweden

[∥]Department of Biophysics, Graduate School of Science, Kyoto University, Kyoto 606-8502, Japan

Supporting Information

ABSTRACT: Molecular cluster ions $H^+(H_2O)_n$, $H^+(pyridine)(H_2O)_n$, $H^+(pyridine)_2(H_2O)_n$, and $H^+(NH_3)(pyridine)(H_2O)_n$ (n = 16−27) and their reactions with ammonia have been studied experimentally using a quadrupole-time-of-flight mass spectrometer. Abundance spectra, evaporation spectra, and reaction branching ratios display magic numbers for $H^+(NH_3)(pyridine)(H_2O)_n$ and $H^+(NH_3)(pyridine)_2(H_2O)_n$ at n = 18, 20, and 27. The reactions between $H^+(pyridine)_m(H_2O)_n$ and ammonia all seem to involve intracluster proton transfer to ammonia, thus giving clusters of high stability as evident from the loss of several water molecules from the reacting cluster. The pattern of the observed magic numbers suggest that $H^+(NH_3)(pyridine)(H_2O)_n$ have structures consisting of a $NH_4^+(H_2O)_n$ core with the pyridine molecule hydrogen-bonded to the surface of the core. This is consistent with the results of high-level ab initio calculations of small protonated pyridine/ammonia/water clusters.

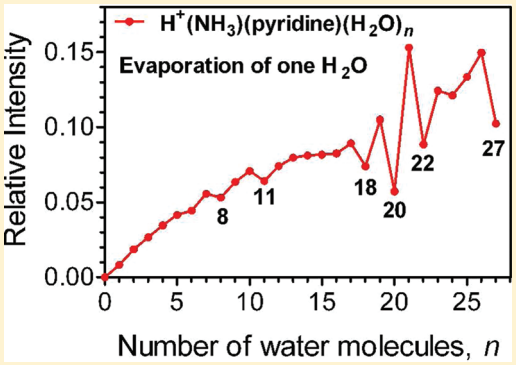

INTRODUCTION

Kinetic models[1] predict protonated water clusters containing ammonia and pyridine to be present in the troposphere at concentrations of ~10^2 cm^{-3}. Such clusters are conveniently produced in the laboratory by electrospray ionization[2,3] but have, to this date, not been identified in ground-based field measurements. However, isolated protonated amines, such as ammonia, pyridine, lutidine, and picoline, have all been observed in atmospheric mass spectrometry measurements,[4−8] but it remains unclear if these protonated amines originate from water clusters that have undergone complete water loss prior to detection or if they exist in the free form in the troposphere.

Protonated water clusters containing amines are also of interest from a fundamental point of view. In the isolated gas phase, the basicity of a given compound is described by its proton affinity (PA); in aqueous solution, it is described by the pK_B value, and the intrinsic basicity is severely moderated by the complex interactions between the molecule and a large number of surrounding water molecules.[9−12] Valuable insights into the solvent effects can be obtained by studying water clusters of the compound. In particular, the interactions between the molecule and water can be studied as a function of cluster size by the controlled step-by-step addition of single water molecules.

In 1973, Lin was the first to observe that, for protonated water clusters, $H^+(H_2O)_n$, some cluster sizes, in particular n = 21, are significantly more abundant than their nearest neighbors, n = 19, 20, 22, 23.[13] Kassner and Hagen described such values of n as "magic numbers" in analogy with the term used in nuclear physics.[14] The underlying thermodynamic stabilization factors are still under discussion. In the case of $H^+(H_2O)_{21}$, it was suggested by Kassner and Hagen that the stabilization is due to an energetically favorable molecular arrangement consisting of a network of 20 water molecules forming a dodecahedral sphere enclosing a hydronium ion. More recently, computational evidence has modified this view, supporting a distorted dodecahedron structure with the proton embedded in the surface rather than being in the interior,[15,16] a point of view that is supported by the observation of distinct IR spectral features.[17−19] Temperature and entropy factors steering the detailed water evaporation dynamics are also known to be significant in determining cluster structure.[20]

Received: March 5, 2012
Revised: May 3, 2012
Published: May 3, 2012

   dx.doi.org/10.1021/jp3021326 | J. Phys. Chem. A 2012, 116, 4902−4908

We have recently studied water clusters containing ammonia and water clusters containing pyridine,[2,3] demonstrating size-dependent hydron (H/D) exchange upon reaction with heavy water. In this article, we present new experimental and computational results with the aim of better understanding the structure of these clusters in relation to the well-described water clusters. Our primary goal was to obtain information on the localization of the excess proton and the nitrogen containing molecules within the clusters.

EXPERIMENTAL METHODS

The experiments were performed applying a modified quadrupole-time-of-flight mass spectrometer (QTOF 2, Micromass/Waters, Manchester UK). The cluster ions were produced from aqueous solutions at atmospheric pressure by electrospray ionization (ESI), and thereafter entered the high vacuum part of the instrument. Three solutions were used: 2.5 mM pyridine for producing $H^+(H_2O)_n$ and $H^+(pyridine)_m(H_2O)_n$ ions, 1.54 M NH_3 for producing $H^+(NH_3)_2(H_2O)_n$ ions, and a mixture of 2.5 mM pyridine and 30 mM NH_3 for producing $H^+(pyridine)_m(H_2O)_n$ and $H^+(NH_3)(pyridine)_m(H_2O)_n$ ions. For abundance spectra, the quadrupole was operated in RF-only mode prior to detection. The QTOF operating parameters (the electrospray voltage, gas flows, and the kinetic energy of the ions passing the collision cell) were varied to produce a cluster distribution with high abundance in the region of interest. For reactivity studies, the quadrupole mass filter (set to better than unit resolution) allowed for selection of single-sized clusters based on their mass-to-charge ratio m/z. Downstream from the quadrupole mass filter the size-selected clusters entered the collision cell, where they were brought to interact with gas phase ammonia at center-of-mass (COM) energies of 8 kJ mol^{-1} (0.085 eV). The reaction products were analyzed using a reflectron time-of-flight (TOF) mass analyzer with a resolution, $m/\Delta m$, of about 5000 (full-width-half-height). The ammonia was introduced into the collision cell through an ultra-high vacuum leak-valve. In order to ensure approximately single collision conditions, the ammonia pressure was adjusted to result in ≤10% ion−neutral collisions, which corresponded to an ammonia pressure of about 10^{-5} mbar. Reference measurements were performed by registering the cluster ion $H^+(pyridine)(H_2O)_{11}$ signal at regular intervals during the experiments to ensure that the reactant gas pressure was constant. For each measurement, a corresponding background measurement was collected with an empty collision cell. Reagents used in the experiments were H_2O (no. 95270 for HPLC, Fluka), pyridine (99.5%, BDH Chemicals Ltd.), NH_3 (99.96%, AGA), and 25% NH_3 (aq) (pro analysi, Merck).

COMPUTATIONAL METHODS

The quantum chemical study included localization of minimum energy structures of isomeric $H^+(NH_3)(pyridine)(H_2O)_n$ with n = 1−4 and calculation of the corresponding electronic energies and Gibbs free energies. Two sets of geometries were investigated: one with the proton located at the pyridine molecule (pyridinium ion) and one with an ammonium core ion, i.e., $(NH_3)(pyridineH^+)(H_2O)_n$ and $(NH_4^+)(pyridine)(H_2O)_n$, respectively. The calculations were performed using the quantum chemistry programs Gaussian09,[21] CP2K,[22] Turbomole,[23,24] and Spartan.[25]

Initial conformational sampling was done using a script described by Ortega et al.[26] The script uses single molecule geometries (given as input) as building blocks to generate a desired number of geometries containing the given number of molecules. The generation of geometries is random within the limits of cluster definitions: the generated configurations are always true clusters according to the Stillinger criterion,[27] i.e., each molecule has at least one neighbor within a predefined radius. Each configuration is checked for uniqueness to avoid calculating the same structure more than once. The script then calculates single point energies for each configuration using the CP2K program and picks a given number of lowest energy geometries. For each value of n (from one to four), we created 10 000 $(NH_3)(pyridineH^+)(H_2O)_n$ configurations, calculated the energies with DFTB,[28] and picked the 50 with the lowest energy. Finally, all configurations were subjected to visual inspection. For each value of n, several geometries were picked as initial geometries for further calculation based on the number and types of hydrogen bonds in the cluster as well as the arrangement of the molecules within the cluster. Since protonated pyridine, H_2O and NH_3 were used as the building blocks during the initial conformational sampling (based on the higher gas-phase PA of pyridine), and since the DFTB optimization did not result in any proton transfers between the protonated pyridine and ammonia, additional geometries were also constructed by hand to represent initial geometries for the higher level calculation clusters.

The so selected initial geometries were then optimized with Gaussian09 employing the widely used hybrid density functional B3LYP[29] with a 6-31G++(2df,2pd) basis set.[30,31] Single-point energies for the optimized geometries were calculated using Turbomole 6.3 employing F12 explicitly correlated second order Møller−Plesset theory with resolution of the identity (RI) approximation, RI-MP2-F12.[32,33] The basis set used was cc-pVDZ-F12, and this basis set was also used for the auxiliary basis set (for which the alias cc-pVDZ-F12 points to the aug-cc-pwCVTZ cbas basis set) and for the complementary auxiliary basis set[34,35] (for cbas, see refs 36 and 37; for cabs, see ref 38). With the F12 method, we are able to get close to the basis set limit even with a relatively small basis set such as cc-pVDZ-F12.[39] Finally, the Gaussian09 program employing the B3LYP/6-31G++(2df,2pd) method were used to calculate thermal corrections to the Gibbs free energy at 298.15 K and 1 atm reference pressure, as well as to probe the proton transfer energy barrier by performing a relaxed scan of the proton transfer from protonated pyridine to NH_3 and from NH_4^+ to pyridine in a $H^+(pyridine)(NH_3)(H_2O)_3$ cluster. In the relaxed scan, the cluster geometry is optimized after each step and only the scanned parameter, in this case the distance of the proton from its initial position, is kept constant in each geometry step. The geometry chosen for proton transfer from protonated pyridine to NH_3 was the only local minimum geometry found in which a $(NH_3)(pyridineH^+)(H_2O)_3$ cluster had the NH_3 molecule situated between the H_2O molecules and the protonated pyridine molecule. The geometry chosen for the proton transfer from NH_4^+ to pyridine was the global minimum geometry for a $(NH_4^+)(pyridine)(H_2O)_3$. The relaxed scans started from these optimized geometries, and the distance between the proton and the initial cation was increased by 0.035 Å during a total of 18 steps.

Binding energies for both $(pyridineH^+)(NH_3)(H_2O)_n$ and $(pyridine)(NH_4^+)(H_2O)_n$ were calculated with respect to the lowest-energy configuration (with and without Gibbs free energy correction) of the isolated gas-phase monomers: $H^+(pyridine)$, NH_3, and H_2O.

dx.doi.org/10.1021/jp3021326 | J. Phys. Chem. A 2012, 116, 4902−4908

EXPERIMENTAL RESULTS

Figure 1 shows a typical abundance mass spectrum (QTOF) obtained from an aqueous solution of 30 mM NH_3 and 2.5 mM

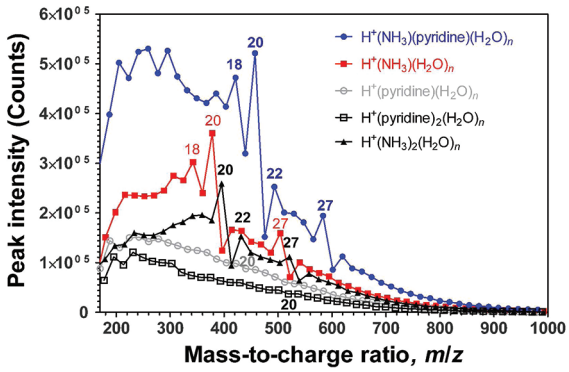

Figure 1. Abundance spectrum obtained from a solution with 30 mM NH_3 and 2.5 mM pyridine. Integer numbers in the figure correspond to the number of water molecules in the cluster. The signal intensity for clusters $H^+(NH_3)(pyridine)(H_2O)_n$, $H^+(pyridine)(H_2O)_n$, and $H^+(pyridine)_2(H_2O)_n$ have been multiplied by 9, 1.5, and 4, respectively. The abundance spectrum for $H^+(NH_3)_2(H_2O)_n$ was obtained in a separate measurement from a 1.54 M NH_3 solution.

pyridine. The spectrum contains signals resulting from the clusters $H^+(NH_3)(H_2O)_n$, $H^+(pyridine)(H_2O)_n$, $H^+(pyridine)_2(H_2O)_n$, and $H^+(NH_3)(pyridine)(H_2O)_n$. Other clusters are also present but are omitted for clarity. In agreement with previous studies,[3,40,41] magic number clusters are observed for $H^+(NH_3)(H_2O)_n$ with n = 18, 20, and 27 and are followed by peaks of lower intensity. For $H^+(pyridine)(H_2O)_n$ and $H^+(pyridine)_2(H_2O)_n$, no obvious magic numbers can be discerned, in agreement with our recently published study.[2] Clusters containing both ammonia and pyridine, $H^+(NH_3)(pyridine)(H_2O)_n$, show magic numbers for n = 18, 20, and 27, i.e., for the same number of water molecules as the $H^+(NH_3)(H_2O)_n$ clusters. In addition, the peak for n = 22 also shows enhanced abundance. Also included in Figure 1 is an abundance spectrum for $H^+(NH_3)_2(H_2O)_n$ clusters obtained from a 1.54 M NH_3 solution. Also for these clusters, magic numbers are found for n = 20, 22, and 27 in agreement with the studies by Schmidt et al. and Shinohara et al.[40−42] We need to emphasize that, while the overall envelope of the observed distributions are sensitive to the operating parameters, the positions of local maximum and minimum abundances, and thereby the magic numbers, are not.

Figure 2 shows the relative amount of evaporation of one water molecule from $H^+(NH_3)(pyridine)(H_2O)_n$ clusters as a function of cluster size during passage from the quadrupole to the detector; the corresponding time window is 148 μs for n = 1 and 161 μs for n = 27. The general trend is that evaporation increases with cluster size, in agreement with previous studies for $H^+(H_2O)_n$, $H^+(NH_3)(H_2O)_n$, and $H^+(pyridine)_m(H_2O)_n$ with m = 1−3.[2,3] Evaporation of one H_2O is suppressed for the magic number clusters, n = 18, 20, and 27, and enhanced for the preceding clusters, n = 19 and 21. In addition, evaporation is suppressed for n = 8, 11, and 22 (although more weakly for the former two), also in accord with the abundance spectrum. Evaporation of ammonia and pyridine is almost absent for all cluster sizes (less than 0.1% for ammonia and less than 0.01% for pyridine).

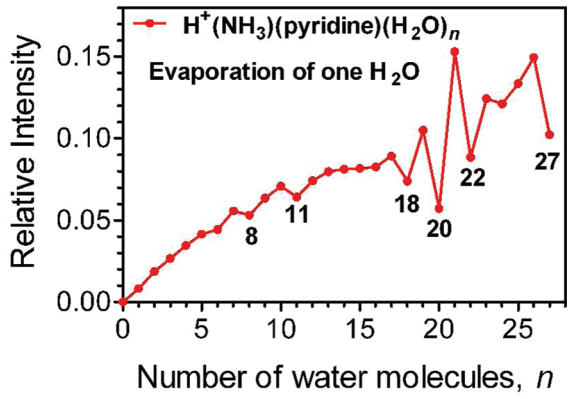

Figure 2. Intensity of the signal resulting from evaporation of one water molecule from $H^+(NH_3)(pyridine)(H_2O)_n$ during flight through an empty collision cell.

The measured branching ratios for reaction with NH_3 can be seen in Figure 3a−d for the clusters $H^+(H_2O)_n$, $H^+(pyridine)(H_2O)_n$, $H^+(pyridine)_2(H_2O)_n$, and $H^+(NH_3)(pyridine)(H_2O)_n$ for n = 16−27. In Figure 3e−f, the corresponding branching ratios are shown corrected for evaporation of water prior to reaction (the correction procedure is described by Ryding et al.;[43] see the Supporting Information for a graphical illustration of the corrections made). The collision energy in the center-of-mass frame (E_{COM}) was in all cases 8 kJ mol^{-1}. For all cluster ions, the loss of pyridine upon reaction with NH_3 is negligible (less than 0.016% and not included in the figure). Instead, NH_3 is incorporated into the cluster, and essentially, only water molecules evaporate.

As seen in Figure 3e, the reaction of $H^+(H_2O)_n$ mainly results in pick-up of NH_3 and subsequent loss of two or three H_2O. The branching ratios are significantly enhanced for reaction channels leading to the magic cluster ion $H^+(NH_3)(H_2O)_{20}$, for example, both $H^+(H_2O)_{22}$ and $H^+(H_2O)_{23}$ mainly give $H^+(NH_3)(H_2O)_{20}$ upon reaction with ammonia. However, we notice that, even though the cluster $H^+(NH_3)(H_2O)_{18}$ is somewhat pronounced in Figure 1, no indication of a particular preference for its formation from any $H^+(H_2O)_n + NH_3$ can be seen in the branching ratios in Figure 3e.

From Figure 3b−c,f−g, it is evident that the reactions between ammonia and the clusters $H^+(pyridine)(H_2O)_n$ and $H^+(pyridine)_2(H_2O)_n$ have almost identical size dependence regarding the number of water molecules lost in the reaction. The formation of $H^+(NH_3)(pyridine)_m(H_2O)_{n-1}$ is significant for 16 < n < 20. This is also seen for n < 16 in a recently published paper.[43] The product ion $H^+(NH_3)(pyridine)_m(H_2O)_{n-2}$ is the main product for both of the cluster types, $H^+(pyridine)(H_2O)_n$ and $H^+(pyridine)_2(H_2O)_n$, in the present size range n = 16−27. It is also the main product for all n below 16 as previously reported.[43] However, exceptionally high branching rations are found for reaction channels producing $H^+(NH_3)(pyridine)_m(H_2O)_{18}$, $H^+(NH_3)(pyridine)_m(H_2O)_{20}$, and $H^+(NH_3)(pyridine)_m(H_2O)_{22}$, i.e., for the channels producing the magic numbers found in Figures 1 and 2.

For $H^+(NH_3)(pyridine)(H_2O)_n$ (n = 16−27) reacting with NH_3, the incorporation of NH_3 is followed by the loss of one or two H_2O as seen in Figure 3d,h. This is in agreement with observations of the same reaction for smaller cluster ions of this type ($n \leq 15$).[43] Furthermore, we note that reaction channels producing $H^+(NH_3)_2(pyridine)(H_2O)_{18}$, $H^+(NH_3)_2(pyridine)$-

dx.doi.org/10.1021/jp3021326 | J. Phys. Chem. A 2012, 116, 4902−4908

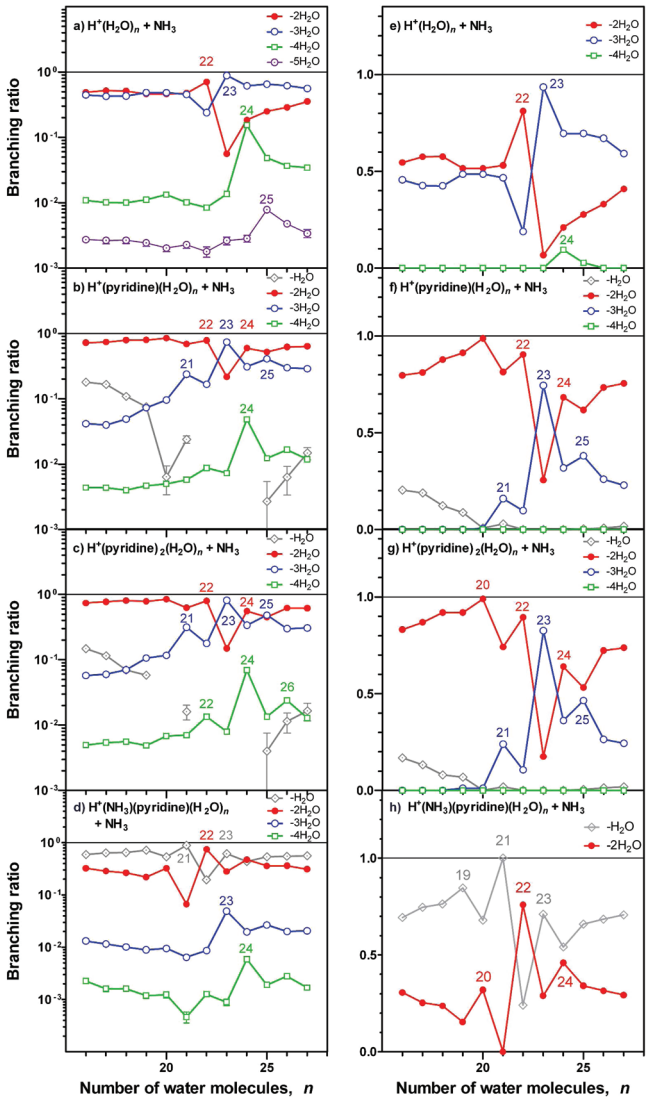

Figure 3. Branching ratios for the reactions of $H^+(pyridine)_m(H_2O)_n$ (m = 0–2) and $H^+(NH_3)(pyridine)(H_2O)_n$ with NH_3 at E_{COM} = 8 kJmol^{-1}. The number of water molecules, n, in the parent cluster ion is indicated for the reaction channels with particularly high branching ratios. Error bars representing one standard deviation due to count statistics are included for all data points in panels a–d.

$(H_2O)_{20}$, and $H^+(NH_3)_2(pyridine)(H_2O)_{22}$ all have very high branching ratios.

COMPUTATIONAL RESULTS

The geometries of the clusters of lowest Gibbs energy are shown in Figure 4. Separation energies and separation standard state Gibbs energies (T = 298.15 K, P = 1 atm) for the minimum energy structures found for the clusters $(NH_3)(pyridineH^+)(H_2O)_n$ and $(NH_4^+)(pyridine)(H_2O)_n$, respectively, are given in Figure 5 (data given in Supporting Information, Table S1). Taken together, the results show that, in the cluster having one water molecule, n = 1, the extra proton is preferably attached to pyridine, whereas for n = 3 or 4, it clearly prefers ammonia, thus having the $(H_2O)_n(NH_4^+)(pyridine)$ structure. For clusters containing two water molecules, protonation at ammonia is preferred, but the Gibbs energy of the pyridine protonated form is only 4 kJ mol^{-1} higher. If this value is taken literally, it means that both

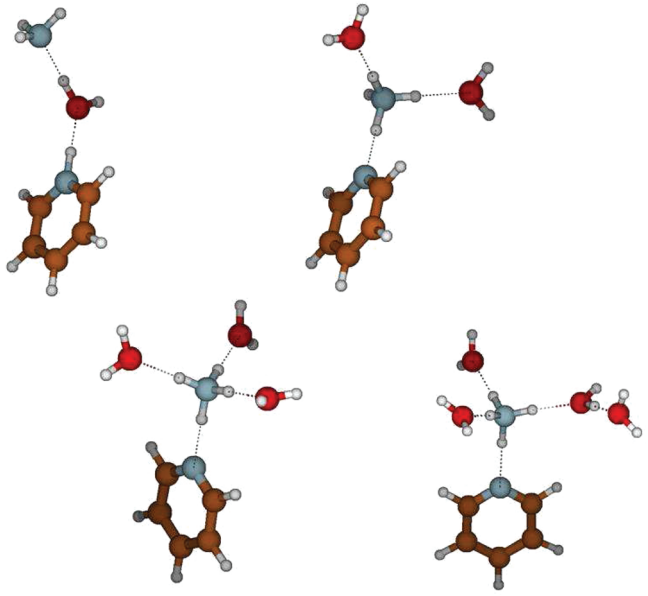

Figure 4. Geometries of the clusters of lowest Gibbs energy.

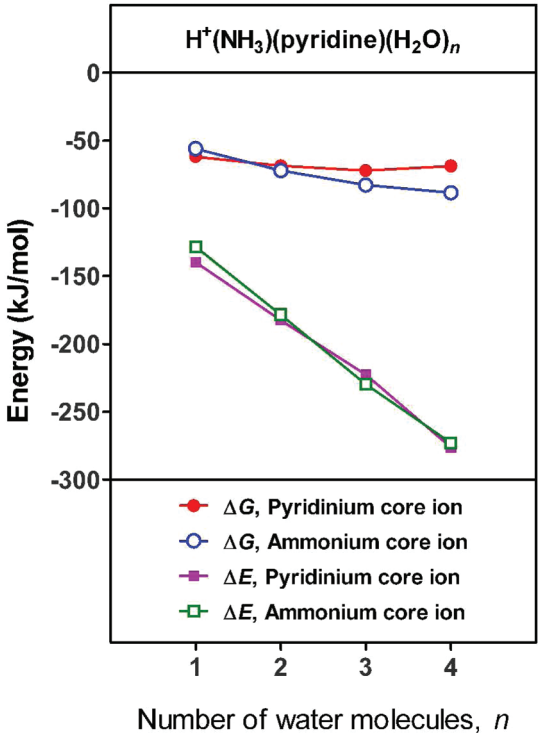

Figure 5. Separation energies, ΔE, and separation Gibbs energies (T = 298.15 K, P = 1 atm), ΔG, with respect to complete dissociation into the isolated molecular components for $H^+(NH_3)(pyridine)(H_2O)_n$ clusters with pyridinium and ammonium core ions, respectively. The reference molecular components are in all cases water, ammonia, and protonated pyridine.

forms are significantly populated at all relevant temperatures; it probably also implies effective proton mobility between the two nitrogen sites. Local minimum-energy cluster-structures of the type $(NH_3)(pyridineH^+)(H_2O)_{3-4}$ were also found but are of higher relative energy.

As can be seen from Figure 4, the ammonium moiety of $(pyridine)(NH_4^+)(H_2O)_{2-4}$ forms a direct hydrogen bond to

dx.doi.org/10.1021/jp3021326 | J. Phys. Chem. A 2012, 116, 4902–4908

the nitrogen of pyridine. In (pyridineH^+)(H_2O)(NH_3), the pyridinium and the NH_3 both form hydrogen bonds to the intermediate H_2O molecule. In our simulations, if water molecules were initially positioned between an ammonium molecule and a pyridine molecule, the proton transferred spontaneously from ammonia to pyridine during geometry optimization, and the end result would be a pyridinium core. Interestingly, however, if the initial configuration has its pyridinium-hydrogen bridging to ammonia, the occurrence or nonoccurrence of spontaneous proton transfer depends on the degree of water solvation at the ammonia molecule. For example, an ammonia molecule initially forming hydrogen bonds to three water molecules does attract the proton, while an ammonia molecule only involved in hydrogen bonding to one water or group of waters (the other two positions being free) do not. These two situations are illustrated in Figure 6.

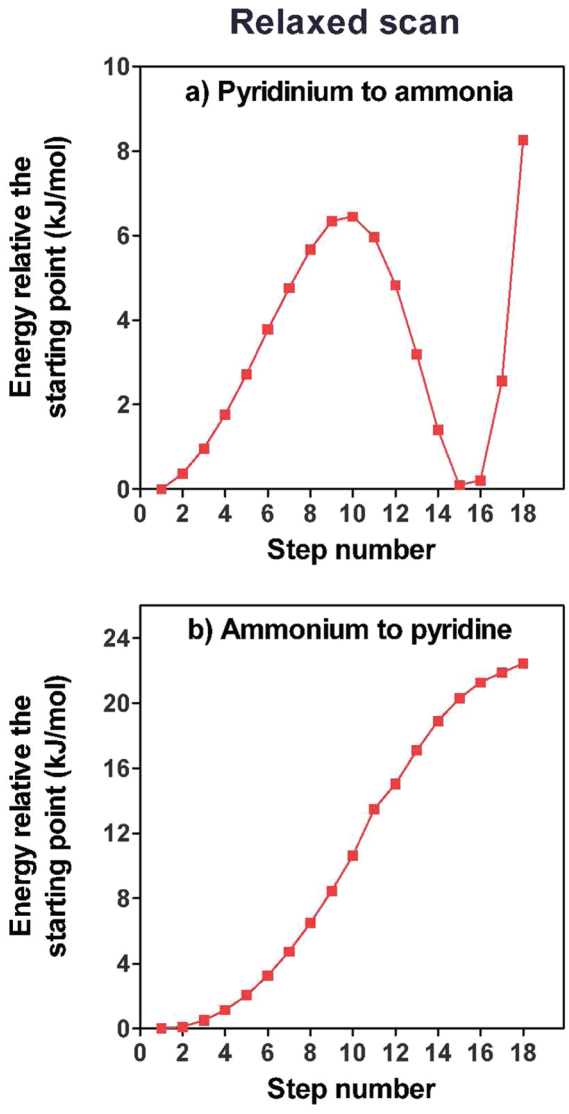

Figure 6. Result of the B3LYP/6-31G++(2df,2pd) relaxed scan (a total of 18 steps) for proton transfer in isomeric (NH_3)(H^+)-(pyridine)(H_2O)$_3$ clusters. For each step, the distance between the proton and the starting position was increased by 0.035 Å and the geometry was then fully optimized keeping this distance constant: (a) transfer from pyridinium to ammonia, and (b) transfer from ammonium to pyridine.

The upper panel shows a simulation of proton transfer from pyridine to ammonia starting from [pyridineH^+···NH_2–H···–OH_2···(OH_2)$_2$], while the lower panel shows proton transfer from ammonia to pyridine starting from [pyridine···$^+$H–NH_3···(OH_2)$_3$]. The initial geometries for the two simulations, as well as the geometries for the step 15 of proton transfer from pyridinium to ammonia and the final step (step 18) of proton transfer from ammonium to pyridine, are shown in Figure 7.

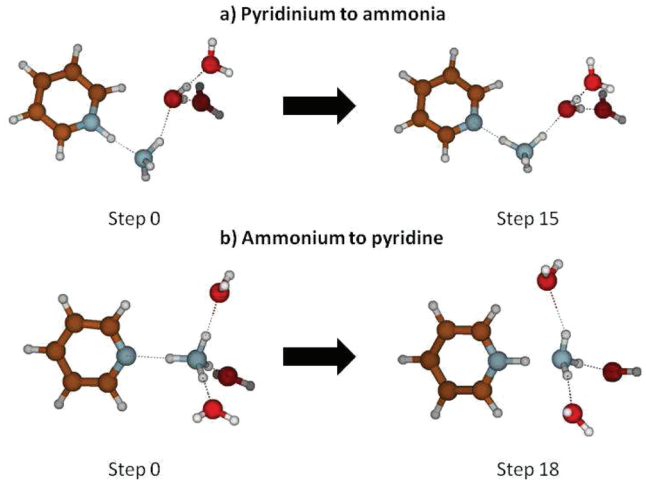

Figure 7. Geometries for the B3LYP/6-31G++(2df,2pd) relaxed scan for proton transfer in isomeric (NH_3)(H^+)(pyridine)(H_2O)$_3$ clusters. (a) Step 0 shows the initial geometry from which the relaxed scan in question was started. Step 15 shows the geometry of the local minima (which can be seen in Figure 6a) for the proton transfer from pyridinium to ammonia. (b) Step 18 shows the geometry of the final step of the relaxed scan for the proton transfer from ammonium to pyridine (Figure 6b).

The barrier height for the transfer from pyridinium to ammonia is 6 kJ mol^{-1} and the two minima, having pyridinium and ammonium cores, respectively, are almost equal in energy with pyridinium being slightly more energetically favorable. The energy difference is negligible, being only 0.1 kJ mol^{-1}. In any case, this barrier is too low to significantly hinder proton motion at any relevant temperature. In summary, the preference of ammonium rather than pyridinium cores in the larger clusters is intimately connected to efficient solvation of the former. For pyridinium, there is only one site for hydrogen bond donation; in ammonium, there are four.

Our calculations do not indicate magic number behavior in cluster stabilities for clusters containing only 1–4 H_2O molecules.

■ DISCUSSION AND CONCLUSIONS

Pure protonated water clusters, $H^+(H_2O)_n$, tend to give away two or three water molecules in approximately equal abundance upon reaction with ammonia (Figure 3). This corresponds to the release of approximately 60 kJ mol^{-1}, if one roughly accounts for three broken hydrogen bonds. If one or two pyridine molecules are present in protonated water clusters, the typical loss is two water molecules, corresponding to a release of 40 kJ mol^{-1}. Protonated water clusters containing both ammonia and pyridine favor loss of one water molecule upon the addition of ammonia, indicating almost thermoneutral reactions.

dx.doi.org/10.1021/jp3021326 | J. Phys. Chem. A 2012, 116, 4902–4908

In experiments in which the reactivity of water-containing clusters ($H^+(H_2O)_n$, $H^+(NH_3)(H_2O)_n$, and $H^+(pyridine)_m(H_2O)_n$, $m = 1-3$) with D_2O was investigated, one water molecule is typically lost subsequent to the addition of the heavy water molecule.[2,3,44] This is easily understood on the basis of thermochemistry since the reaction energy for $H^+(H_2O)_n + D_2O \rightarrow H^+(D_2O)(H_2O)_n + H_2O$ is practically zero, owing to the identical number of O−H and O−D bonds on reactant and product sides. The 60 kJ mol^{-1} higher energy that is released in the reaction with ammonia can be accounted for by assuming that the proton ends up on ammonia. The exact energy associated with this process does of course depend upon cluster size and the degree of ion hydration. It is relevant that the difference in *PA* between H_2O and NH_3 is 163 kJ mol^{-1} in the isolated gas phase, while it is only 52 kJ mol^{-1} in bulk water.[45] The latter value, corresponding to the expected asymptotic value for very large clusters, is seen to be in good accord with our rather primitive estimate.

The proton affinity of pyridine in the isolated gas phase is 76 kJ mol^{-1} higher than that of ammonia,[46] while in aqueous solution, it is 22 kJ mol^{-1} lower.[45] Now, assuming that the proton is attached to pyridine in $H^+(pyridine)(H_2O)_n$, as indicated in earlier work,[2] and transferred to the picked-up ammonia, this may account for the lower tendency for loss of three vs two water molecules compared to pure water clusters. As seen for $H^+(pyridine)_2(H_2O)_n$, a second pyridine present does not result in any significant difference in the ratio $[-3H_2O]/[-2H_2O]$.

It is highly significant that adding ammonia to clusters that already contain ammonia, $H^+(NH_3)(pyridine)(H_2O)_n$, results in a weakly exothermic reaction, evident from the tendency of losing only one and, to a lesser extent, two water molecules. This fact is consistent with the proton being already attached to the NH_3, in full accord with our quantum chemical calculations.

On the basis of these considerations, it appears safe to conclude that protonated water clusters containing one ammonia and one pyridine molecule have the general formula $(pyridine)(NH_4^+)(H_2O)_n$, stabilized by hydration of the ammonium core. A possible exception is $n = 1$. For small clusters (except $n = 1$), our quantum chemical calculations indicate that the pyridine is in contact with the ammonium ion core via a hydrogen bond, although this is not necessarily the case for larger clusters. From a previous study, it is known that protonated mixed ammonia/water clusters always have a NH_4^+ core with water and ammonia competing on an almost equal footing for the positions in the first solvation shell.[47] It is also known that, with the exception of the nitrogen site, the pyridine molecule interacts weakly with water molecules in $H^+(pyridine)_m(H_2O)_n$ clusters and will reside in the periphery of a water cluster.[2]

Not the least, this study reveals very interesting information on magic numbers. Both the reactivity data and the evaporation data are consistent in showing that ions of the general formula $H^+(NH_3)_l(pyridine)_m(H_2O)_n$ demonstrate particularly high stability relevant to their nearest neighbors for $n = 20$. This feature is evident for all clusters containing ammonia and is noticeably absent for $H^+(pyridine)_m(H_2O)_n$, i.e., clusters not containing ammonia. We consider this observation in light of our well-supported hypothesis that protonated water clusters containing ammonia have a common NH_4^+ core. The ammonium core appears to function as a template in structuring the surrounding waters, giving rise to a common $NH_4^+(H_2O)_n$ motif seen most clearly for $n = 20$ but also for $n =$ 18, 22, and 27. In the case of $H^+(NH_3)(H_2O)_n$, this is a well-known phenomenon.[3,16,42,48] On this basis, the remaining question is how the remaining pyridine and ammonia molecules bind to the indicated $NH_4^+(H_2O)_n$ structural motif.

On the basis of a reactivity study and a spectroscopic study, it has been inferred that the NH_4^+ ion in a $NH_4^+(H_2O)_{20}$ cluster is found at the surface, perhaps with one dangling N−H bond,[42,48] while one computational study suggests that the NH_4^+ ion is located in the cluster center but that its position is temperature dependent.[16] If NH_4^+ is situated at the cluster surface, it may provide a ligand binding without altering the cluster structure. Schmidt et al.[42] suggested that the two ammonia molecules in $H^+(NH_3)_2(H_2O)_{20}$ are bonded together by a proton bond bridge, thus corresponding to $NH_4^+(H_2O)_{20}$ with NH_3 dangling outside the cluster by means of a hydrogen bond to NH_4^+. It seems likely that pyridine behaves in the same manner, and one may envisage a general situation with a $NH_4^+(H_2O)_n$ core having tag-along pyridine and ammonia molecules attached to the cluster surface. Also in $H^+(pyridine)_m(H_2O)_n$ clusters, not containing ammonia, it seems most likely that the pyridines will be in surface positions due to the large hydrophobic part of the molecule. In these clusters, the proton will be at one of the pyridine molecules, while the other will be unprotonated.[2] It is interesting that, in reactions between clusters containing two pyridine molecules, we observe water loss upon the addition of ammonia but essentially no pyridine loss, indicating that pyridine is more strongly bonded than water. This is also in good qualitative agreement with the observations made by Viggiano et al.[49] that pyridine adds efficiently to $H^+(NH_3)_m(H_2O)_n$ ($m + n \leq 5$) clusters, which is followed by evaporation of water and ammonia.

■ ASSOCIATED CONTENT

Ⓢ Supporting Information

Graphical representation of the changes made when going from the uncorrected branching ratios (Figure 3a−d) to the corrected ones (Figure 3e−h), i.e., the part of each product peak that can safely be assumed to originate from the parent ion reactant; table containing the values displayed in Figure 5 for the separation energies (ΔE) and separation Gibbs energies (ΔG). This material is available free of charge via the Internet at http://pubs.acs.org.

■ AUTHOR INFORMATION

Corresponding Author

*E-mail: mauritz.ryding@kjemi.uio.no (M.J.R.); einar.uggerud@kjemi.uio.no (E.U.).

Notes

The authors declare no competing financial interest.

■ ACKNOWLEDGMENTS

This work was supported by the Swedish Research Council, the Norwegian Research Council by the Grant No. 179568/V30 to the Centre of Theoretical and Computational Chemistry through their Centre of Excellence program, the Nanoparticle in Interactive Environments platform at the Faculty of Science at University of Gothenburg, the Philosophical Faculty donation fund at the University of Gothenburg, the Academy of Finland (Center of Excellence program project number 1118615, LASTU program project number 135054), and ERC project 257360-MOCAPAF.

REFERENCES

(1) Beig, G.; Brasseur, G. P. *J. Geophys. Res., [Atmos.]* **2000**, *105*, 22671−22684.
(2) Ryding, M. J.; Zatula, A. S.; Andersson, P. U.; Uggerud, E. *Phys. Chem. Chem. Phys.* **2011**, *13*, 1356−1367.
(3) Andersson, P. U.; Ryding, M. J.; Sekiguchi, O.; Uggerud, E. *Phys. Chem. Chem. Phys.* **2008**, *10*, 6127−6134.
(4) Eisele, F. L. *J. Geophys. Res., [Atmos.]* **1988**, *93*, 716−724.
(5) Perkins, M. D.; Eisele, F. L. *J. Geophys. Res., [Atmos.]* **1984**, *89*, 9649−9657.
(6) Schulte, P.; Arnold, F. *Geophys. Res. Lett.* **1990**, *17*, 1077−1080.
(7) Junninen, H.; Ehn, M.; Petaja, T.; Luosujarvi, L.; Kotiaho, T.; Kostiainen, R.; Rohner, U.; Gonin, M.; Fuhrer, K.; Kulmala, M.; Worsnop, D. R. *Atmos. Meas. Tech.* **2010**, *3*, 1039−1053.
(8) Ehn, M.; Junninen, H.; Petaja, T.; Kurten, T.; Kerminen, V. M.; Schobesberger, S.; Manninen, H. E.; Ortega, I. K.; Vehkamaki, H.; Kulmala, M.; Worsnop, D. R. *Atmos. Chem. Phys.* **2010**, *10*, 8513−8530.
(9) Munson, M. S. B. *J. Am. Chem. Soc.* **1965**, *87*, 2332−2336.
(10) Brauman, J. I.; Riveros, J. M.; Blair, L. K. *J. Am. Chem. Soc.* **1971**, *93*, 3914−3916.
(11) Aue, D. H.; Webb, H. M.; Bowers, M. T. *J. Am. Chem. Soc.* **1976**, *98*, 318−329.
(12) Alder, R. W. *Chem. Rev.* **1989**, *89*, 1215−1223.
(13) Lin, S. S. *Rev. Sci. Instrum.* **1973**, *44*, 516−517.
(14) Kassner, J. L.; Hagen, D. E. *J. Chem. Phys.* **1976**, *64*, 1860−1861.
(15) Hodges, M. P.; Wales, D. J. *Chem. Phys. Lett.* **2000**, *324*, 279−288.
(16) Anick, D. J. *J. Chem. Phys.* **2010**, *132*, 164311/1−164311/12.
(17) Miyazaki, M.; Fujii, A.; Ebata, T.; Mikami, N. *Science* **2004**, *304*, 1134−1137.
(18) Shin, J. W.; Hammer, N. I.; Diken, E. G.; Johnson, M. A.; Walters, R. S.; Jaeger, T. D.; Duncan, M. A.; Christie, R. A.; Jordan, K. D. *Science* **2004**, *304*, 1137−1140.
(19) Wu, C.-C.; Lin, C.-K.; Chang, H.-C.; Jiang, J.-C.; Kuo, J.-L.; Klein, M. L. *J. Chem. Phys.* **2005**, *122*, 074315−074319.
(20) Hansen, K.; Andersson, P. U.; Uggerud, E. *J. Chem. Phys.* **2009**, *131*, 124303/1−124303/7.
(21) Frisch, M. J.; Trucks, G. W.; Schlegel, H. B.; Scuseria, G. E.; Robb, M. A.; Cheeseman, J. R.; Scalmani, G.; Barone, V.; Mennucci, B.; Petersson, G. A.; Nakatsuji, H.; Caricato, M.; Li, X.; Hratchian, H. P.; Izmaylov, A. F.; Bloino, J.; Zheng, G.; Sonnenberg, J. L.; Hada, M.; Ehara, M.; Toyota, K.; Fukuda, R.; Hasegawa, J.; Ishida, M.; Nakajima, T.; Honda, Y.; Kitao, O.; Nakai, H.; Vreven, T.; Montgomery, J. A., Jr.; Peralta, J. E.; Ogliaro, F.; Bearpark, M.; Heyd, J. J.; Brothers, E.; Kudin, K. N.; Staroverov, V. N.; Kobayashi, R.; Normand, J.; Raghavachari, K.; Rendell, A.; Burant, J. C.; Iyengar, S. S.; Tomasi, J.; Cossi, M.; Rega, N.; Millam, J. M.; Klene, M.; Knox, J. E.; Cross, J. B.; Bakken, V.; Adamo, C.; Jaramillo, J.; Gomperts, R.; Stratmann, R. E.; Yazyev, O.; Austin, A. J.; Cammi, R.; Pomelli, C.; Ochterski, J. W.; Martin, R. L.; Morokuma, K.; Zakrzewski, V. G.; Voth, G. A.; Salvador, P.; Dannenberg, J. J.; Dapprich, S.; Daniels, A. D.; Farkas, O.; Foresman, J. B.; Ortiz, J. V.; Cioslowski, J.; Fox, D. J. *Gaussian 09*, revision A.01; Gaussian, Inc.: Wallingford, CT, 2009.
(22) CP2K Developers Group. *CP2K*, 2011. http://cp2k.berlios.de/.
(23) Ahlrichs, R.; Baer, M.; Haeser, M.; Horn, H.; Koelmel, C. *Chem. Phys. Lett.* **1989**, *162*, 165−169.
(24) *Turbomole 6.3*; Turbomole GmbH: Karlsruhe, Germany, 2011. http://www.turbomole.com.
(25) Wavefunction, Inc. *Spartan '06 Windows*; Wavefunction, Inc.: Irvine, CA, 2006. http://wavefun.com.
(26) Ortega, I. K.; Kupiainen, O.; Kurtén, T.; Olenius, T.; Wilkman, O.; McGrath, M. J.; Loukonen, V.; Vehkamäki, H. *Atmos. Chem. Phys.* **2012**, *12*, 225−235.
(27) Stillinger, J. F. H. *J. Chem. Phys.* **1963**, *38*, 1486−1494.
(28) Elstner, M.; Porezag, D.; Jungnickel, G.; Elsner, J.; Haugk, M.; Frauenheim, T.; Suhai, S.; Seifert, G. *Phys. Rev. B: Condens. Matter Mater. Phys.* **1998**, *58*, 7260−7268.
(29) Becke, A. D. *J. Chem. Phys.* **1993**, *98*, 5648−5652.
(30) Francl, M. M.; Pietro, W. J.; Hehre, W. J.; Binkley, J. S.; Gordon, M. S.; DeFrees, D. J.; Pople, J. A. *J. Chem. Phys.* **1982**, *77*, 3654−3665.
(31) Frisch, M. J.; Pople, J. A.; Binkley, J. S. *J. Chem. Phys.* **1984**, *80*, 3265−3269.
(32) Klopper, W.; Samson, C. C. M. *J. Chem. Phys.* **2002**, *116*, 6397−6410.
(33) Tew, D. P.; Klopper, W. *J. Chem. Phys.* **2005**, *123*, 074101−074113.
(34) Peterson, K. A.; Adler, T. B.; Werner, H.-J. *J. Chem. Phys.* **2008**, *128*, 084102−12.
(35) Bischoff, F. A.; Wolfsegger, S.; Tew, D. P.; Klopper, W. *Mol. Phys.* **2009**, *107*, 963−975.
(36) Hattig, C. *Phys. Chem. Chem. Phys.* **2005**, *7*, 59−66.
(37) Weigend, F.; Kohn, A.; Hattig, C. *J. Chem. Phys.* **2002**, *116*, 3175−3183.
(38) Yousaf, K. E.; Peterson, K. A. *J. Chem. Phys.* **2008**, *129*, 184108−184117.
(39) Bachorz, R. A.; Bischoff, F. A.; Glöß, A.; Hättig, C.; Höfener, S.; Klopper, W.; Tew, D. P. *J. Comput. Chem.* **2011**, *32*, 2492−2513.
(40) Shinohara, H.; Nagashima, U.; Nishi, N. *Chem. Phys. Lett.* **1984**, *111*, 511−513.
(41) Shinohara, H.; Nagashima, U.; Tanaka, H.; Nishi, N. *J. Chem. Phys.* **1985**, *83*, 4183−4192.
(42) Schmidt, M.; Masson, A.; Brechignac, C.; Cheng, H. P. *J. Chem. Phys.* **2007**, *126*, 154315/1−154315/5.
(43) Ryding, M. J.; Jonsson, Ã. M.; Zatula, A. S.; Andersson, P. U.; Uggerud, E. *Atmos. Chem. Phys.* **2012**, *12*, 2809−2822.
(44) Zatula, A. S.; Andersson, P. U.; Ryding, M. J.; Uggerud, E. *Phys. Chem. Chem. Phys.* **2011**, *13*, 13287−13294.
(45) Shriver, D. F.; Atkins, P. W.; Langford, C. H. *Inorganic Chemistry*; Oxford University Press: Oxford, UK, 1990.
(46) Lide, D. R. *CRC Handbook of Chemistry and Physics*; Lide, D. R., Ed.; Taylor and Francis: Boca Raton, FL, 2006.
(47) Hvelplund, P.; Kurten, T.; Stochkel, K.; Ryding, M. J.; Nielsen, S. B.; Uggerud, E. *J. Phys. Chem. A* **2010**, *114*, 7301−7310.
(48) Diken, E. G.; Hammer, N. I.; Johnson, M. A.; Christie, R. A.; Jordan, K. D. *J. Chem. Phys.* **2005**, *123*, 164309/1−164309/7.
(49) Viggiano, A. A.; Morris, R. A.; Dale, F.; Paulson, J. F. *J. Geophys. Res., [Atmos.]* **1988**, *93*, 9534−9538.